Egyptian Journal of Chemistry

http://ejchem.journals.ekb.eg/

An Unusual Corrosion Product, Kobyashevite, From Ancient Egyptian Copper Artifacts: Technical Note

Manal A. Maher[a]*, Yussri Salem[b]

[a] Post graduate Studies College of Nanotechnology, Cairo University; Computed Tomography X-Ray unit, Cairo Egyptian Museum, Ministry of Tourism and Antiquities, Egypt;

[b]Department Conservation, Faculty of Archaeology, South Valley University, Qena 83523, Egypt.

ABSTRACT

Kobyashevite is one of the copper sulfates hydroxide hydrate minerals "devilline group". It forms as a thin crust in the calcite and gypsum veins and takes a flower-like morphology. Kobyashevite was identified as a synthesized corrosion product in the laboratory studies on the copper samples in a humid air containing SO_2, while it did not identify in the archeological metals' corrosion studies before. The case study is a set of copper model tools from Cairo Egyptian Museum dated back to Dynasty Xth (2134-2050 BC). It was not undergone of any conservation processes before; this gives an authenticity of all taken samples and subsequently accurate results. X-ray fluorescence, Scanning electron microscopy-energy dispersive X-ray spectroscopy, X-ray diffraction and Raman spectroscopy were carried out in order to identify the corrosion products. Besides that, a potable digital microscopy was used to examine the morphology of the outer surface corrosion layer. The present study identified the unusual mineral of copper sulfates hydroxide hydrate 'Kobyashevite' as a natural corrosion product for the first time on the archeological field; and suggested its formation due to exposure the case study to uncontrolled long–term humid storage environment contaminated with a high concentration of sulfur gases.

Keywords: Kobyashevite; atmospheric pollution; sulfur dioxide; copper corrosion products; copper model tools

1. INTRODUCTION

Seven copper sulfates minerals with OH groups; H_2O molecules; and without other species-defining cations or anions were geologically identified before such: Langite $Cu_4(SO_4)(OH)_6 \cdot 2H_2O$; Montetrisaite $Cu_6(SO_4)(OH)_{10} \cdot 2H_2O$; Posnjakite $Cu_4(SO_4)(OH)_6 \cdot H_2O$; Ramsbeckite $Cu_{1.5}(SO_4)_4(OH)_{22} \cdot 6H_2O$; Redgillite $Cu_6(SO_4)(OH)_{10} \cdot H_2O$; Schulenbergite $Cu_7(SO_4)_2(OH)_{10} \cdot 3H_2O$; Wroewolfeite $Cu_4(SO_4)(OH)_6 \cdot 2H_2O$. Besides all these copper sulfates minerals, there is other copper sulfates mineral called "Kobyashevite" which also belongs to the "devilline group" minerals but it is very rare formation in the earth crust. Originally, Kobyashevite formed in the Kapital'naya mine at South Urals, Russia, as thin crusts in the calcite and gypsum veins there. It also is formed as a supergene mineral in the cavities of quartz veins' with chalcopyrite and pyrite [1].

Langite, posnjakite, and wroewolfeite were identified as natural corrosion products on the surface of some outdoor renascence copper and bronze statues located in the urban environments. Different studies explained that the formation reason of these copper sulfates corrosion products is a chemical reaction between the copper-based artifacts and the sulfur gases. Since the sulfur gases are essential pollutants to form the acidic rains in the industrial and urban cities [2-6].

The ideal chemical formula of a "Kobyashevite" is written as $Cu_5(SO_4)_2(OH)_6 \cdot 4H_2O$ or $Cu_{2.5}(OH)_3SO_4 \cdot 2H_2O$. It is characterized with a bluish-green to turquoise color, vitreous Luster, 2½ Mohs

_____

hardness and has {010} distinct Cleavage [7]. Kobyashevite was identified as a corrosion product only in the laboratory studies and it was not identified as a natural corrosion product on any archaeological copper artifacts before [8]. Strandberg [1] identified a "Kobyashevite" in her laboratory study of the atmospheric corrosion of copper and bronze in a humid air containing sulfur dioxide gas. Also, she identified it another time in her study of the effect of NaCl in a combination with O_3 and SO_2 gases on the atmospheric corrosion of copper [9].

The ancient Egyptian civilization has one of the oldest and the most important metallic heritages in the entire ancient world [10]. The majority of this great ancient Egyptian heritage was excavated in two different burial environments; direct and indirect. The 'direct' is the artifacts had been buried directly in the soil, so it was in a direct contact with the soil components. While the 'indirect' is the objects had been located in the tomb's underground chambers [11]. Thus, in the two burial environments, the ancient metals artifacts were affected by different corrosive factors such amount/type of soluble salts (anions), soil water content, soil aeration, soil pH, presence of microorganisms or organic compounds, surrounded gases, humidity and temperature [12, 13]. So that, there is a variety of corrosion products could be formed on the ancient copper-based alloys according to the deterioration factors of the buried or surrounded environment. In this regard, there are many archaeological copper-based artifacts studies analyzed and identified different copper corrosion products. These studies introduced more deeply understanding to the nature of different copper corrosion products on the archaeological copper-based alloys and its formation mechanisms, stratification structures. Also, it gave important information about the new undefined copper corrosion products which rarely formed on the archaeological copper-based alloys [14-20].

The present research identifies the rare copper sulfates corrosion product 'Kobyashevite", for the first time in the archaeological metals studies, on ancient Egyptian copper model-tools from Cairo Egyptian Museum.

2. MATERIALS AND METHODS

The case study is a set of hammered copper model tools from Cairo Egyptian Museum collection. It was dated back to the Dynasty Xth, 1st Intermediate Period (2134-2050 BC). It was found in the TOMB OF KHENNU AND APA-EM-SA-F (289) in the south of

Memphis 'Saqqara', and it was excavated by Quibell during the excavation year (1906-1907) [21]. The study set consists of twenty-five objects including three axes; fourteen chisels, seven adzes, and one dead-end needle [see Figure 1]. All the set objects were registered at Cairo Egyptian museum archives under the number JE39230. It was stored in a small carton box in the base of the showcase L in the room no.32 at the upper floor of the museum. Fortunately, the case study group had never been undergone any treatment process before whether during the excavation or its storage time in the museum. So, it was remained without any addition of any cleaning and/or conservation materials.

Different microscopes were used in order to examine the morphology and stratigraphy of the corrosion layers. Firstly, Dnt DigiMicro Mobile USB/TFT Portable Digital Microscope 500X, 5.0 Megapixel was used to examine different corrosion products phases on the outer surface of all the case study objects. Secondly, Scanning Electron Microscopy attached with Energy-Dispersive X-ray Spectroscopy (SEM-EDS) was used in order to get the elemental analysis of different corrosion products layers through the cross-section sample. The elemental analysis mapping of the cross-section was also achieved, which has great information about the elements distribution through of the corrosion layers and the positions of all soil inclusions, contaminants, etc. In order to achieve SEM-EDS examination, a very small sample (2×2 mm) was taken from the chisel J by use jewelry saw [Figure 1 - the red dashed lines pointed out the location of the cross-section sample]. Memorable, SEM-EDS sample must have a metal core covered with a thick of corrosion crusts. This cross-section sample was prepared by molding in a cold-setting resin, and after its complete solidification, it was grinded and polished via different coarseness emery papers varies (800–4000 grit) and diamond paste (1 and 3 μm) to obtain a very smooth polished surface [22]. The microscopic examination of the polished cross-section was achieved without any coating and etching solution. The examination was achieved on a SEM/EDS apparatus Model FEI INSPECT S50, EDS Quantax Bruker in El-Tabbin Institute for Metallurgical Studies in Cairo, Egypt, under operating conditions: low vacuum mode at 0.8 torr, and the backscatter electron images (BSE) have been gotten at acceleration voltage 25.0 kV with a backscattered detector working distance at 5 mm and spot size 6.
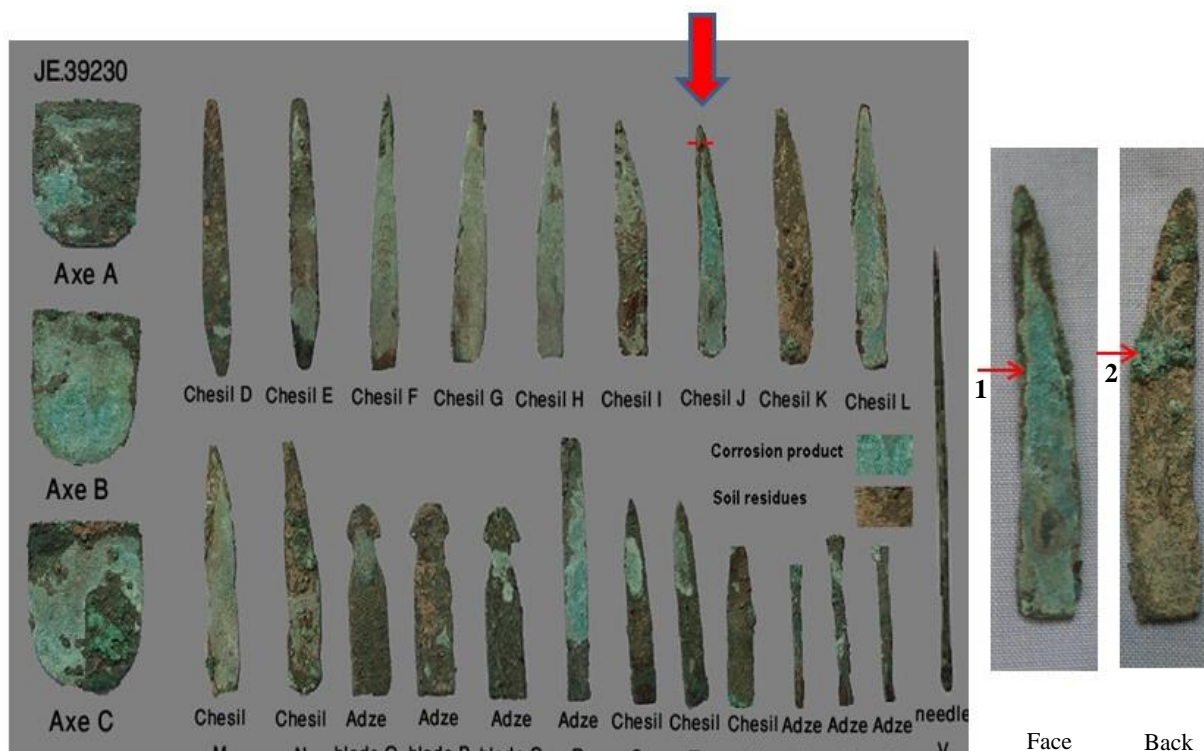
_____

Figure 1. Copper model tools with magnify of the chisel J and illustration a kobyashevite corrosion product in the bluish-green color in the face and back sides of the chisel

X-ray fluorescence elemental analysis was carried out for the bluish-green corrosion product sample (no.1) from the face surface of the Chesil J [see red arrow in the Figure 1]. The analysis carried out by X-ray fluorescence system (ED-XRF) (JEOL JSX 3222 model), under operating conditions : X-ray generator is 5 to 50 KV and 0.01 to 1.0 mA tube current, X-ray tube is end window type and Be 127 µm thick.

X-ray diffraction (XRD) also was used to identify the chemical composition of the corrosion products. For this purpose, two powder corrosion product samples were scratched from the face and back sides of the chisel J surface [see Figure 1 - the red arrows pointed out the locations of the two scratched powder corrosion samples]. In order to achieve XRD analysis, the corrosion samples were highly grinded by using an agate pestle mortar to be a very fine powder. The grinded samples were performed on XRD equipment PAN analytical X'pert PRO Diffractometer model in the Central Metallurgical Research and Development Institute, El-Tabbin, Cairo, Egypt, under operating conditions : secondary monochromator with a Cu-Kα1 target, λ 0.1542 nm, and operated generator power 45 kV and 40 mA, scanning step rate is 0.05°/s, incidence angles 2Ө start from 0° to 80°. The resulted mineralized phases were identified by matching the d-spacing values of the samples by JCPDS (Joint Committee for Powder Diffraction Studies) and AMCSD (American Mineralogist Crystal Structure Database) identification cards.

Finally, the polished cross-section sample was investigated via Raman spectroscopy in order to determine the micro-stratigraphic of the inner corrosion layers and identify its compounds. Raman spectroscopy is a typical characterization procedure for the metals patinas and inner corrosion layers [23]. Raman measurements were achieved by using the dispersive Raman microscope model Senterra of Bruker Company in the Egyptian Petroleum Research Institute (EPRI) Cairo, Egypt. The spectra were acquired at room temperature via a laser beam wavelength 785 nm, power 25 MW, and aperture setting 50×1000 µm. The cross-section was scanned twice and the spectrometer calibration was obtained from a silicon crystal in which the Raman signal is at 520.5 cm^{-1}.

3. RESULTS

3.1. PORTABLE DIGITAL MICROSCOPY

Figure 2 (a-f) shows the different copper corrosion products and soil residues on the outer surface of the chisel J. Whereas, Figure 2 (a, b) showed a Kobyashevite in a turquoise-blue phase mixed with a pale blue corrosion product "Paratacamite". While in Figure 2 (c) illustrates a bluish-green phase of Kobyashevite in another part on the chisel J. Figure 2 (d) shows the cracked stress corrosion which is probably as a result of the existence of the residual stresses due to the cold working forming process of the object. That is, this artifact probably didn't exposure to a sufficient annealing process or any other surface heat treatments during its manufacture. So, the artifact tried to lose the internal residual stresses which due to the hammering process as corrosion products forms of the metal [22]. Finally, Figure 2 (e, f) illustrates the soil residues mixed with green and pale green corrosion products.

3.2. X-RAY FLUORESCENCE

Figure 3 shows XRF elemental analysis pattern of the bluish-green corrosion product sample (no.1). The figure shows that the sample consists of Cl (10.72), **S (6.56)**, K (0.11), As (0.63), Mn (0.04) and, Cu (81.94) elements. This indicates that the corrosion sample consists of chlorides, sulfides and/or sulfates copper corrosion products. The same sample was analyzed also by XRD and Raman spectroscopy to confirm the presence of these different copper corrosion products phases.

3.3. SCANNING ELECTRON MICROSCOPY-ENERGY DISPRESIVE X-RAY

SEM-EDS examination was performed to study the stratification of corrosion products layers and detected their elemental analysis. Figure 4 (a) illustrates the elemental analysis of the outer and under-surface corrosion layers in the studied cross-section sample. While, EDS analysis (spots 1, 2) illustrates the percentage values of Cu, C, O, Cl, **S** elements in the
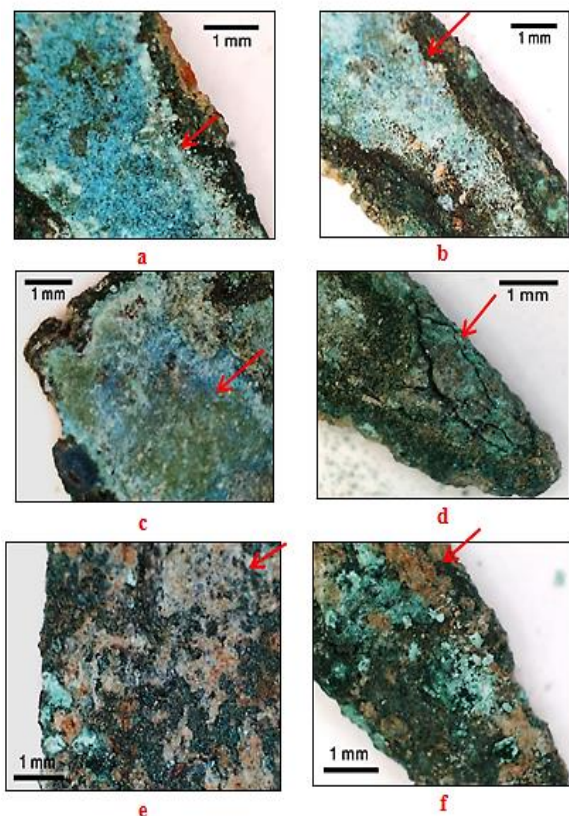
_____

Figure 2. Portable Stereomicroscope images reveal different copper corrosion products on the chisel J's outer surface

under-surface and outer corrosion layers of the cross-section respectively which indicate to the presence of copper carbonates, oxides, chlorides, sulfates and/or sulfides corrosion products in the both corrosion layers. Whereas, the sulfur element was detected in the under-surface corrosion layer only (spot 1) in value 4.89%. While, it was not detected in the outer corrosion layer (spot 2) which is rich by chlorine element (Cl). The presence of the chlorine element in the outer and under-surface corrosion layers in values 13.95%, 6.54% respectively is confirmation to affect the chisel J by bronze disease. Figure 4 (b) illustrates the distribution mapping micrographs of all the resulted elements which was detected by EDS analysis through the studied cross-section. In the micrographs, the white arrows pointed to the presence of a sulfur element in the under-surface corrosion layer. So that, EDS and its distribution elemental mapping confirm to the presence of a sulfur element only in the under-surface corrosion layer and it isn't existent in the outer corrosion surface layer in the cross-section.

3.4. X-RAY DIFFRACTION

Figure 5 (a, b) illustrates XRD patterns of two corrosion powder samples were scratched from the both surfaces of the chisel J. The patterns illustrates that the two samples consist of copper oxides and chlorides which are common corrosion products on the most copper-based artifacts. While still there are some peaks in the XRD patterns that were unidentified.
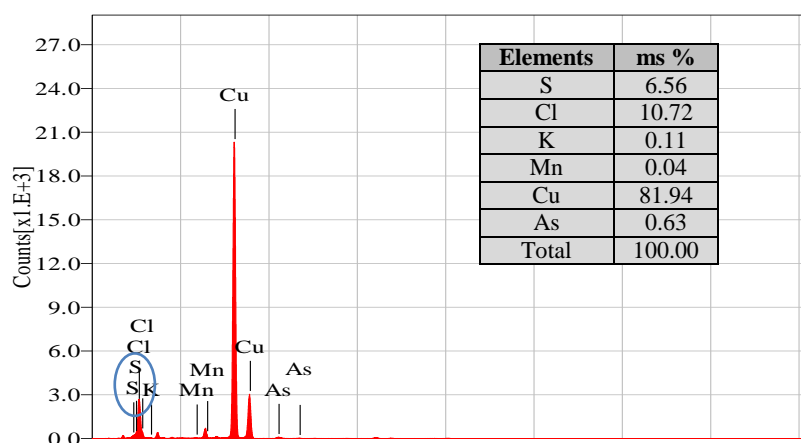

Elements	ms %
S	6.56
Cl	10.72
K	0.11
Mn	0.04
Cu	81.94
As	0.63
Total	100.00

Figure 3. XRF pattern of the elemental analysis of the powder bluish-green corrosion product sample (no.1)
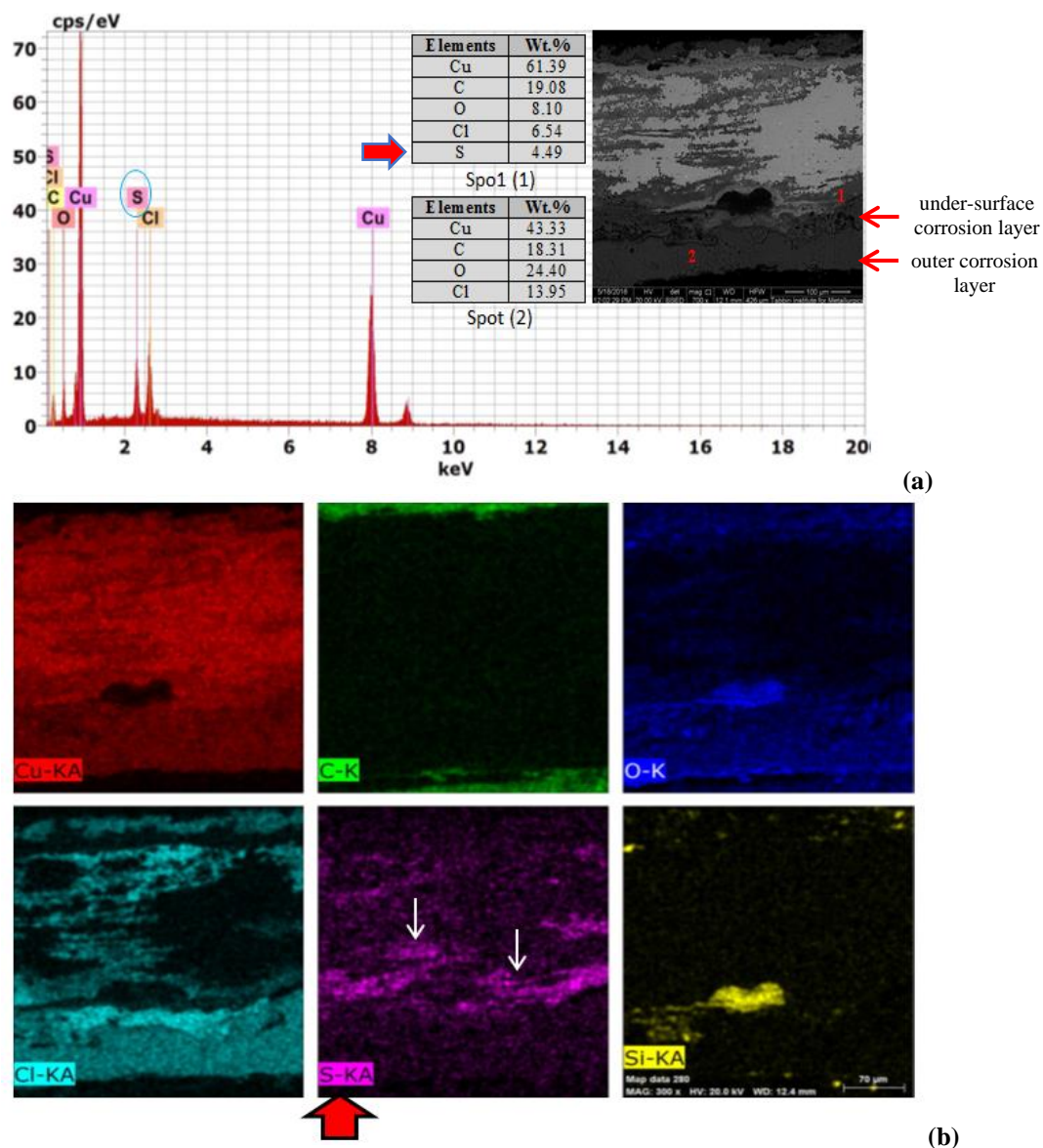
_____

(a)

(b)

Figure 4. (a) EDS elemental analysis illustrated the presence of the sulfur element in the under-surface corrosion layer, (b) the mapping micrographs of elements distribution through the cross-section sample of the chisel J.

2.1. So, these unidentified peaks indicated to the presence other corrosion product (s) which is (are) not common copper corrosion products and unidentified before. While, the detection of sulfur element in the elemental analysis of this sample either in X-ray Fluorescence or in the energy-dispersive X-ray spectroscopy (Figure 3, Figure 4a), is a confirmation to the presence of copper sulfides and/or sulfates corrosion products in this sample. Thus, the d-values for these unidentified XRD peaks were matched by the search-match program supported (JCPDS) and (AMCSD) cards of all copper sulfides and sulfates minerals whether were identified as corrosion products or not [1, 7, 8]. This important matching process revealed that these unidentified X-ray diffraction peaks belong to one of a rare copper sulfates hydroxide hydrate called "Kobyashevite". Table 1 illustrates the agreement matching of the two powder corrosion samples with a Kobyashevite mineral which identified by ASTM card no. (041-00067). It is obvious the strongest diffraction reflection peak corresponding to Kobyashevite in the two samples appear at (2Θ 16.05°± 0.05) which is the main peak and fingerprint of the Kobyashevite compound.

Table *2* [10] illustrates the identified copper sulfates, sulfides and chlorides minerals - whether identified as corrosion products or not - which were used in the matching of XRD analysis of the two corrosion samples.
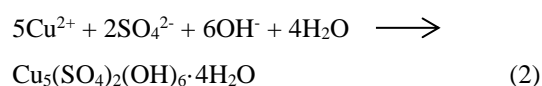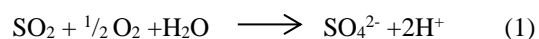
3.5. RAMAN SPECTROSCOPY

The pervious different analytical procedures XRF, SEM-EDS, elemental mapping and XRD identified the existence of the sulfur element and a kobyashevite corrosion product on the outer corrosion layer and in the under-surface corrosion layer of the chisel J. Raman spectroscopy was achieved also on a cross-section sample in order to identify the penetration of sulfur element and subsequently the formation of a Kobyashevite corrosion product in the internal core metal of the studied object. Figure 6 illustrates the Raman patterns of the two spots in the cross-section of the chisel J. In the first spot, the figure shows the presence of a Kobyashevite at wavenumbers (221, 425, 980 and 1135 cm^{-1}); beside the detection of nantokite corrosion product at wavenumbers (260,

While, in the second spot, a Kobyashevite was detected at wavenumbers (450, 975 and 1135 cm^{-1}); beside the detection other copper corrosion products of nantokite at wavenumbers (262, 400, 688, 811 cm^{-1}) [26,27], Malachite at wavenumbers (352, 532, 765, 1072, 1212, 1360, 1460, 1502, 2881 cm^{-1}) [28,29] and finally paratacamite at wavenumbers (143, 262, 400, 738 cm^{-1}) [25, 30-32].

4. DISCUSSION

The formation of a Kobyashevite, like other copper sulfates hydroxide hydrates corrosion products, can be attributed to the presence of a sulfur element in the surrounded environment of the copper-based objects [2-6]. Since, during a long burial time in the tomb, the common copper corrosion products such as copper oxides, carbonates, and chlorides were formed on the surface of the case study objects. While, after its excavation and exposed to the open air which contains different pollution elements. It could be possible to form different unusual other copper corrosion products according the type and concentration of the pollution elements in the surrounded environment. Memorable, the case study was stored for a long time up to 110 years in uncontrolled closed environments in the museum. This long storage time, beside to increasing of the humidity in the storage environment and absence of treatment and/or preventive conservation procedures are sufficient reasons to formation different corrosion products on the case study objects.

In this regard, Strandberg [1] explained the formation of a Kobyashevite as a result of direct chemical reactions between the copper metal and sulfur dioxide gas [see the equations (1, 2)]:

$$SO_2 + \tfrac{1}{2}O_2 + H_2O \longrightarrow SO_4^{2-} + 2H^+ \qquad (1)$$

$$5Cu^{2+} + 2SO_4^{2-} + 6OH^- + 4H_2O \longrightarrow$$
$$Cu_5(SO_4)_2(OH)_6 \cdot 4H_2O \qquad\qquad (2)$$

While, Scott [10] explained the formation reason of a Kobyashevite as an intermediate corrosion product phase of the basic corrosion sulfates especially Brochantite.

_____

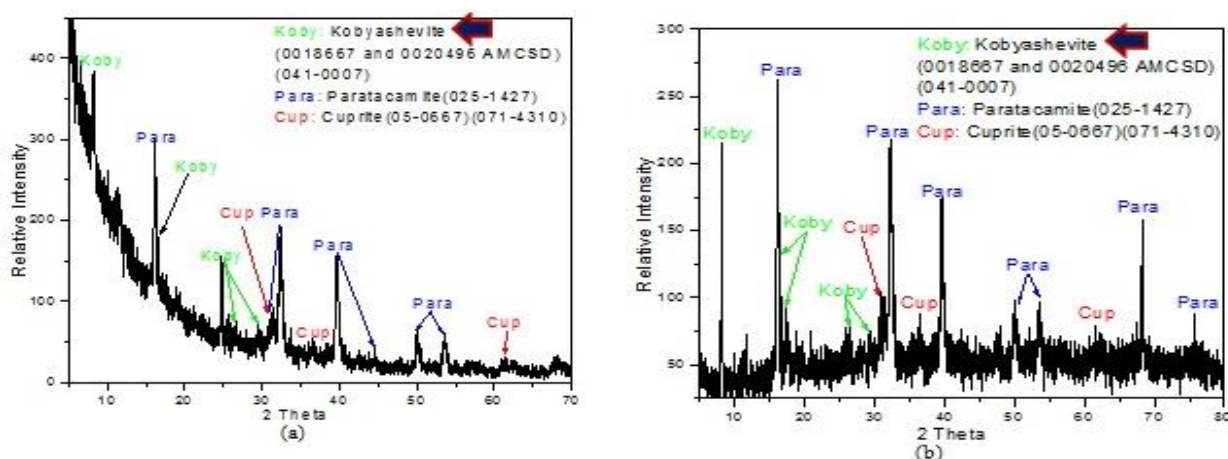400, 612, 678, 840, 812 cm^{-1}) [24,25].

Figure 5. XRD patterns of two corrosion powder samples from the corrosion surface of chisel J of (a) Sample no.1, (b) Sample no.2

Table 1. XRD identification of two corrosion powder samples scratched from the face and back surface of chisel J

	Sample no.1					Sample no. 2			
No.	Pos. [°2Th.]	d-spacing [Å]	Rel. Int. [%]	Koby. (041-00067)	No.	Pos. [°2Th.]	d-spacing [Å]	Rel. Int. [%]	Koby. (041-00067)
1	8.1746	10.81623	56.94	√	1	8.1532	10.82114	8.66	√
2	11.5996	7.62906	46.56		2	10.9204	8.10194	4.95	
3	16.1273	5.46234	100	√	3	11.5030	7.69293	9.45	
4	16.4273	5.34011	42.12		4	16.0493	5.52249	100.00	√
5	24.77	3.58651	50.82	√	5	16.4273			
6	25.95	3.4731	10.47	√	6	17.19			
7	29.51	3.02701	10.47	√	7	17.3447	5.11285	9.50	√
8	31.2391	2.86329	21.58		8	18.8515	4.70746	8.32	
9	32.4808	2.77324	84.32	√	9	20.0408	4.46156	1.81	√
10	36.5579	2.45801	7.09	√	10	20.7304	4.28484	4.92	
11	39.6767	2.27168	77.88	√	11	21.5194	4.09192	2.14	√
12	44.63	2.03039	9.82	√	12	25.7191	3.46393	4.27	
13	50.8271	1.81986	20.79	√	13	26.5362	3.35909	8.87	
14	53.5787	1.70907	24.67	√	14	27.7296	3.21717	3.54	
15	61.59	1.50671	6.55	√	15	28.3845	3.14442	4.68	
16	67.97	1.3792	9.16		16	29.3196	3.04623	7.28	√
					17	31.8441	2.90284	18.12	√
					18	32.1320	2.78574	74.45	√
					19	33.7215	2.65798	2.19	√
					20	36.2766	2.47641	9.35	√
					21	38.3606	2.34654	7.40	√
					22	39.5708	2.27752	56.91	√
					23	42.1229	2.14525	4.71	√
					24	42.9850	2.10420	2.44	√
					25	44.5178	2.03525	4.28	√
					26	47.5950	1.91060	6.10	√
					27	50.0171	1.82361	16.13	
					28	51.9908	1.75893	2.04	√
					29	53.5491	1.71136	14.36	
					30	68.2347	1.37335	47.77	

Table 2. Identified copper sulfates, sulfides and chlorides minerals-whether were defined as corrosion products or not [10]

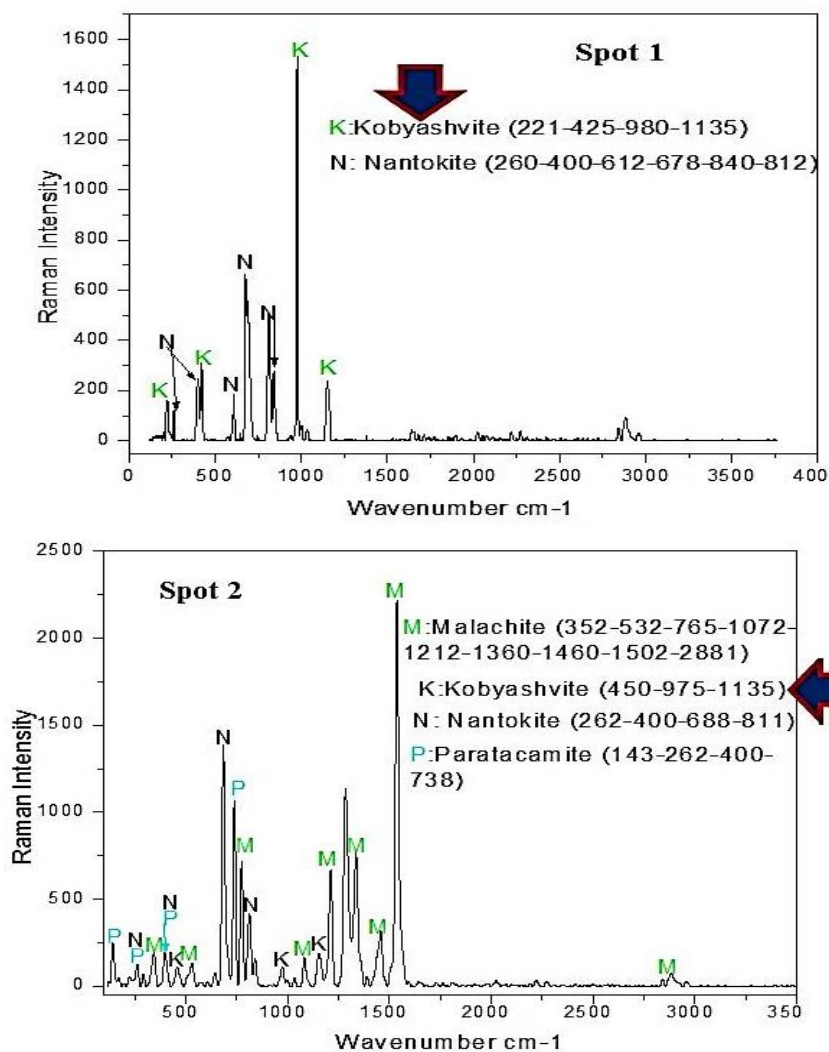| Copper sulfate hydroxides/hydrates		sulfides	chlorides
Brochantite $Cu_4(SO_4)(OH)_6$	**Langite** $Cu_4(SO_4)(OH)_6.2H_2O$	**Covellite** CuS	**Eriochalcite** $CuCl_2.2H_2O$
Antlerite $Cu_3(SO_4)(OH)_4$	**Posnjakite** $Cu_4(SO_4)(OH)_6. H_2O$	**Chalcocite** Cu_2S	**Claringbullite** $Cu_4Cl(OH)_7$
Chalcanthite $CuSO_4.5H_2O$	**Wroewolfeite** $Cu_4(SO_4)(OH)_6.2H_2O$	**Djurleite** $Cu_{31}S_{16}$	**Anthonyite** $Cu(OH,Cl)_2.3H_2O$
Dolerophanite $Cu_2O(SO_4)$	**Redgillite** $Cu_6(OH)_{10}(SO_4).H_2O$	**Villamaninite** CuS_2	**Nantokite** $CuCl$
Bonattite $CuSO_4.3H_2O$	$Cu_3(SO_4)_2(OH)_2.2H_2O$	**Geerite** Cu_8S_5	**Botallackite** $Cu_2Cl(OH)_3$
Chalcocyanite $CuSO_4$		**spionkopite** $Cu_{39}S_{28}$	**Atacamite** $Cu_2Cl(OH)_3$
		yarrowite, Cu_9S_8	**Belloite** $Cu(OH)Cl$
		Roxbyite Cu_9S_5	**Melanothallite** Cu_2Cl_2O
		Anilite Cu_7S_4	**Clinoatacamite** $Cu_2(OH)_3Cl$
		Digenite Cu_9S_5	**Paratacamite** $Cu_2(OH)_3Cl$
			Calumetite $Cu(OH, Cl)_2.2H_2O$

Figure 6. Raman patterns of two spots through the cross-section sample of the chisel J; spot 1 in under-surface corrosion layer, while spot 2 in the outer corrosion layer

However, Scott [10] explanation did not agree the presence of a Kobyashevite on the present case study because Brochantite corrosion product did not detect in any pervious achieved analysis procedures. Thus, the presence of this rare and unusual copper sulfates hydroxide hydrates "Kobyashevite" on the case study can be attributed, according to Strandberg explanation [1], due to a chemical reaction of the copper-based artifacts and the sulfur dioxide pollutant gas during the long uncontrolled storage time in the museum.

Cairo Egyptian museum air contains different pollution gases from indoor and/or outdoor sources. Transportation traffic in The Tahrir Square is an essential source of SO_X gases concentration in the interior environment of Cairo Egyptian museum. Shakour [33,34] measured the concentration of sulfur dioxide gas inside and outside the Cairo Egyptian museum. She detected the average concentration of sulfur dioxide gas reached to 18.7 μg/m^3 inside the museum on the first-floor air where the main entrance of the museum, while its concentration reached to 13.6 μg/m^3 in the second-floor air. Additionally, its concentration reached to 130 μg/m^3 in some days according to the increasing rate of transportation traffic congestion in the Tahrir Square. Memorable, these results of the sulfur dioxide gas average concentration exceeded the maximum permissible whether in the museum's external and/or internal air. Since, the standard levels of indoor pollutants in the museums set by the Canadian Conservation Institute (CCI) is 2.5 μg/m^3 [35], and according to the American National Standard Institute it is 5 μg/m^3 [36]. This limit is more dangerous for most of the museums' artifacts, since it affect in the deterioration of papers, metals, leathers, natural and synthetic fibers...etc [37]. Also, the Cairo Egyptian Museum floors were covered by gray and black vulcanization rubber slabs since the late seventies. These rubber slabs were an essential source of sulfur element indoors the museum which affected dangerously on most museum artifacts. Fortunately, since late 2016, these rubber slabs were partly removed from the most of museum's rooms floors and replaced by more safe floors slabs, this by the financial funding from the European Union (personal communication) [38].

5. CONCLUSION

Kobyashevite is one of copper sulfates hydroxides hydrates corrosion products group, but it is a rarely formation in the nature. It was not identified as a natural corrosion product on any archaeological copper artifacts before. The present study identified a Kobyashevite, as the first time in the archaeological studies, on archaeological copper objects from the Cairo Egyptian Museum Collection. The case study is a model tools set dated back to Dynasty Xth (2134-2050 BC) and was excavated at Saqqara. The study attributed that the reason of the Kobyashevite formation on the case study is a chemical reaction between the case study and sulfur dioxide gases due to its storage for a long time in an uncontrolled humid environment contaminated by sulfur dioxide gases. The essential indoor source of the sulfur dioxide gases inside the Cairo Egyptian museum is covering its floors by vulcanization rubber slabs, besides the transportation traffic outside the museum as outdoor source. Additionally, the most museums' halls museum doesn't equip with a central air condition or air filters for preventing the air pollution gaseous and the solid pollutants from outdoor source. So, it is necessity to remove the vulcanization rubber slabs from all museum halls and replacing by safe floors' slabs for archaeological materials. Also, it is necessity equipping the museum by air filters to preventing the gaseous and solid pollutants.

Reference

[1] Strandberg, H., Langer, V., & Johansson, L. G., Structure of Cu2.5(OH)3SO4·2H2O: a Novel Corrosion Product of Copper. *Acta Chemica Scandinavica*, 49(1), 5-10 (1995). http://actachemscand.org/pdf/acta_vol_49_p0005-0010.pdf

[2] Graedel, T. E., & Franey, J. P., Formation and characteristics of the Statue of Liberty patina, In The Statue of Liberty restoration: proceedings of the Statue of Liberty-today for tomorrow conference, New York, 101-108 (1989) https://en.calameo.com/books/000075335c184bd7c7b68

[3] Stöckle, B., Pöhlmann, G., Mach, M & Snethlage, R., "UNECE international cooperative programme on effects on materials, including historic and cultural monuments", Report no. 5 Corrosion attack on copper and cast bronze, Evaluation after 1 and 2 years of exposure, Bavarian State Conservation Office, Munich, Germany (1991).

[4] Marani, D., Patterson, J. W., & Anderson, P. R., Alkaline precipitation and aging of Cu (II) in the presence of sulfate. Water Research, 29(5), 1317-1326 (1995). https://www.sciencedirect.com/science/article/abs/pii/004313549400286G

[5] Nord, A. G., Tronner, K., & Boyce, A. J., Atmospheric bronze and copper corrosion as an environmental indicator. A study based on chemical and sulphur isotope data. Water, air, and soil pollution journal, 127(1-4), 193-204 (2001).

[6] Selwyn, L. S., Binnie, N. E., Poitras, J., Laver, M. E., & Downham, D. A., Outdoor bronze statues: analysis of metal and surface samples. *Studies in conservation*, 41(4), 205-228 (1996). https://www.tandfonline.com/doi/abs/10.1179/sic.1996.41.4.205

[7] Pekov, I. V., Zubkova, N. V., Yapaskurt, V. O., Belakovskiy, D. I., Chukanov, N. V., Kasatkin, A. V., & Pushcharovsky, D. Y. Kobyashevite, Cu5(SO4)2(OH)6·4H2O, a new devilline-group mineral from the Vishnevye Mountains, South Urals, Russia. *Mineralogy and Petrology*, 107(2), 201-210 (2013). https://link.springer.com/article/10.1007/s00710-012-0236-4

[8] Strandberg, H., & Johansson, L. G., Some aspects of the atmospheric corrosion of copper in the presence of sodium chloride. *Journal of the Electrochemical Society,* 145(4), 1093-1100 (1998).

https://iopscience.iop.org/article/10.1149/1.1838422

[9] Strandberg, H., Role of O[sub 3] in the Atmospheric Corrosion of Copper in the Presence of SO[sub 2]. *Journal of the Electrochemical Society*, 144(7), 2334-2342 (1997). https://www.osti.gov/biblio/533114-role-sub-atmospheric-corrosion-copper-presence-so-sub

[10] Scott, D. A., "Copper and bronze in art: corrosion, colorants, conservation". 1st edition; Getty publications (2002). https://www.getty.edu/conservation/publications_resources/books/copper_bronze_in_art.html

[11] Ogden, J., "Metals", in P.T. Nicholson and I. Shaw, eds, Ancient Egyptian Materials and Technology, Cambridge University Press, Cambridge, 148–176 (2000). http://farlang.com/metals-in-ancient-egypt-jewelry

[12] Angelini, E., Rosalbino, F., GRASSIN, S., Ingo, G. M., & De Caro, T., Simulation of corrosion processes of buried archaeological bronze artefacts. In Corrosion of Metallic Heritage Artefacts (pp. 203-218). Woodhead Publishing (2007). https://www.researchgate.net/publication/279433752_Simulation_of_corrosion_processes_of_buried_archaeological_bronze_artefacts

[13] Oudbashi, O., A methodological approach to estimate soil corrosivity for archaeological copper alloy artefacts. *Heritage Science*, 6(2) 1-15 (2018). https://link.springer.com/article/10.1186/s40494-018-0167-4

[14] Meakin, J. D., Ames, D. L., & Dolske, D. A., Degradation of monumental bronzes. *Atmospheric Environment*. Part B. Urban Atmosphere, 26(2), 207-215 (1992). https://www.sciencedirect.com/science/article/abs/pii/095712729290024M

[15] Ibrahim, A. G. A. A., & Maher, M. AA, Case Study of Copper-Arsenic Ewer from the Egyptian Museum in Cairo, Egypt. *Journal of the General Union of Arab Archaeologists,* 3(3), 1-25 (2018). https://jguaa2.journals.ekb.eg/article_6693.html

_____

[16] Oddy, W.A., Meeks N.D., Unusual phenomena in the corrosion of ancient bronze, *Studies in Conservation 27 (sup1)*, 119-124 (1982).

[17] Fabrizi, M., Ganiaris, H., Tarling, St., Scott, D., The occurrence of Sampleite, A complex copper phosphate, As a corrosion product on copper alloy objects from Memphis, Egypt, *Studies in Conservation* 34: 45-51 (1989).

[18] Thickett, D., and Odlyha, M., Note on the identification of an unusual pale blue corrosion product from Egyptian copper alloy artefacts, *Studies in Conservation* 45 (1) 63-67 (2000).

[19] Zhang X., An unusual corrosion product, Pyromorphite, from a bronze *An*: A technical note, *Studies in Conservation* 47 (1) 76-79 (2002).

[20] InGo, G.M., De Caro, T., Riccucci, C, and Khosroff, S., Uncommon corrosion phenomena of archaeological bronze alloys, *Applied Physics A - Materials Science & Processing* 83 (4), 581-588 (2006). https://link.springer.com/article/10.1007/s00339-006-3534-z

[21] QUIBELL, J. E., "Excavations at Saqqara (1906-1907) with a section on the religious texts". s.l.:LE CAIRE: IMPRIMERIE DE L'INSTITUT FRANCAIS D'ARCHEOLOGIE ORIENTALE. (1908). https://www.persee.fr/doc/jds_0021-8103_1910_num_8_6_3574_t1_0276_0000_1

[22] SCOTT, D. A., "Metallography and Microstructure of Ancient and Historic Metals" (No. 77). s.l.: Los Angeles, CA: The Getty Conservation Institute (1991). https://www.getty.edu/conservation/publications_resources/pdf_publications/pdf/metallography.pdf

[23] BELLOT-GURLet, L., NEFF, D., REGUER, S., MONNIER, J., SAHEB, M., & DILLMANN, P., Raman Studies of Corrosion Layers Formed on Archaeological Irons in Various Media. *Journal of Nano Research*, Issue 8, 147–156 (2009). https://hal.archives-ouvertes.fr/file/index/docid/477440/filename/Bellot-Gurlet-et-al_2009-JNR.pdf

[24] Schindelholz, E. J., Cong, H., Jove-Colon, C. F., Li, S., Ohlhausen, J. A., & Moffat, H. K., Electrochemical aspects of copper atmospheric corrosion in the presence of sodium chloride. *Electrochimica Acta,* 276, 194-206 (2018). https://www.osti.gov/pages/servlets/purl/1444080

[25] Zhang, X., Wallinder, I. O., & Leygraf, C., Mechanistic studies of corrosion product flaking on copper and copper-based alloys in marine environments. *Corrosion Science,* 85, 15-25 (2014). https://www.sciencedirect.com/science/article/pii/S0010938X14001516

[26] Frost, R. L., Williams, P. A., Kloprogge, J. T., & Martens, W., Raman spectroscopy of the copper chloride minerals nantokite, eriochalcite and claringbullite–implications for copper corrosion. Neues Jahrbuch für Mineralogie-Monatshefte, (10), 433-445 (2003). https://eprints.qut.edu.au/23828/1/Raman_spectroscopy_of_the_copper_chloride_minerals_nantokite,_eriochalcite_and_claringbullite.pdf

[27] Frost, R. L., Raman spectroscopy of selected copper minerals of significance in corrosion. Spectrochimica acta Part A: molecular and biomolecular spectroscopy. 59(6), 1195-1204 (2003). https://eprints.qut.edu.au/5413/1/5413.pdf

[28] Inberg, A., Ashkenazi, D., Cohen, M., Iddan, N., & Cvikel, D., Corrosion products and microstructure of copper alloy coins from the Byzantine-period Ma'agan Mikhael B shipwreck, Israel. *Microchemical Journal*, 143, 400-409 (2018). https://www.sciencedirect.com/science/article/abs/pii/S0026265X18307239

[29] Piccardo, P., Mödlinger, M., Ghiara, G., Campodonico, S., & Bongiorno, V., Investigation on a "tentacle-like" corrosion feature on Bronze Age tin-bronze objects. *Applied Physics A,* 113(4), 1039-1047 (2013). https://link.springer.com/article/10.1007/s00339-013-7732-1

[30] Li, S., Teague, M. T., Doll, G. L., Schindelholz, E. J., & Cong, H., Interfacial corrosion of copper in concentrated chloride solution and the formation of

_____

copper hydroxychloride. *Corrosion Science*, 141, 243-254 (2018). https://www.osti.gov/pages/servlets/purl/1485452

[31] Li, S., Teague, M. T., Doll, G. L., Schindelholz, E. J., & Cong, H., Interfacial corrosion of copper in concentrated chloride solution and the formation of copper hydroxychloride. *Corrosion Science*, **141**, 243-254 (2018). https://www.osti.gov/pages/servlets/purl/1485452

[32] Martens, W., Frost, R. L., & Williams, P. A., Raman and infrared spectroscopic study of the basic copper chloride minerals–implications for the study of the copper and brass corrosion and. Neues Jahrbuch für Mineralogie-Abhandlungen: *Journal of Mineralogy and Geochemistry*, **178**(2), 197-215 (2003). https://eprints.qut.edu.au/22212/1/Raman_and_infr ared_spectroscopic_study_of_the_basic_copper_ch loride_minerals.pdf

[33] Shakour, A.A. and El-Taieb, N.M., Air Quality Indoor the Egyptian Museum in Cairo, Bulletin of the National Research Centre, Egypt, 20(4), 415-427 (1995).

[34] El-Taieb, N.M. and Shakour, A.A., Evaluation of air quality indoor the Egyptian Museum in Cairo, Egyptian *Journal of Basic and Applied Sciences*, 18 (8B) 695-704 (2003).

[35] Lafontaine, R. H. "Environmental norms for Canadian museums, art galleries and archives". Art Galleries and Archives Technical Bulletin. CCI, 5, Vol. 1979. No. 5, 1979. https://www.worldcat.org/title/environmental-norms-for-canadian-museums-art-galleries-and-archives/oclc/6901379

[36] ANSI, Particle for Storage of processed safety and photographic film American National Standards Institute, 1981. https://standards.globalspec.com/std/149795/ANSI %20IT9.11

[37] Gibson, L. T., Cooksey, B. G., Littlejohn, D., & Tennent, N. H., Investigation of the composition of a unique efflorescence on calcareous museum artifacts. *Analytica Chimica Acta*, 337(3), 253-264 (1997).

[38] The information is from Dr. Lotfy L. Abdel Hamied, General Director of Archaeological affairs, Cairo Egyptian Museum, LotfyHamied@yahoo.com

مركب "الكوبي اشفيت" Kobyashevite هو واحد من معادن كبريتات النحاسيك القاعدية او ما يطلق عليها "مجموعة معادن الديفيلين". حيث يتكون "الكوبي اشفيت" كقشرة طلاء رقيقة في عروق الكالسيت والجبس وتأخذ بلورته مورفولوجيا تشبه شكل الزهور كما يتراوح لونه بين الأخضر المزرق إلى الأزرق الفيروزي. ولقد تم تصنيعه خلال الدراسات المعملية في هواء جوي رطب محتوي على جزء من المليون من غاز ثانى اكسيد الكبريت. فى حين لم يتم تعيينه من قبل في أى من الدراسات السابقة لصدأ المعادن الأثرية كمركب صدأ طبيعي على الاثار النحاسية.

والقطع الاثرية موضوع البحث عبارة عن مجموعة من الأدوات النموذجية المصنعة من معدن النحاس المكتشفة بمنطقة سقارة والتى تعود الى الاسرة العاشرة من التاريخ الفرعونى والموجودة بالمتحف المصري بالقاهرة. ولحسن الحظ فان القطع موضوع البحث لم تخضع لأي عملية من عمليات الصيانة او التنظيف من قبل مما أعطى دقة عالية فى نتائج تحليل العينات. ولقد تم تحليل عينات الصدأ المأخوذة من الاثر موضوع البحث بواسطة الميكروسكوب الالكترونى الماسح الملحق بوحدة التحليل العنصرى، وأيضاً باستخدام تفلور وحيود الأشعة السينية وأخيراً باستخدام مطياف الرامان وذلك من أجل تحديد مركبات الصدأ الموجودة على سطح الاثر موضوع البحث.

ولقد قامت الدراسة بتعيين مركب "الكوبي اشفيت" لأول مرة فى مجال الاثار كأحد مركبات الصدأ الطبيعية التى يمكن ان تتكون على سطح الاثار النحاسية. ولقد انتهت الدراسة الى أن السبب الرئيسى لتكون مركب صدأ "الكوبي اشفيت" على مجموعة البحث هو نتيجة تعرض القطع الأثرية لبيئة رطبة غير متحكم فيها خلال فترة زمنية طويلة من التخزين بالمتحف فى جو يحتوى على نسبة عالية من غاز ثانى اكسيد الكبريت.

الكلمات المفتاحية: الكوبي اشفيت ؛ تلوث الهواء ؛ مركبات صدأ النحاس ؛ ثانى اكسيد الكبريت؛ نماذج الأدوات النحاسية.